Thermochimica Acta, 121 (1987) 39–49
Elsevier Science Publishers B.V., Amsterdam – Printed in The Netherlands

DIFFERENTIAL SCANNING CALORIMETRY OF THE DOLOMITE–ANKERITE MINERAL SERIES IN FLOWING NITROGEN *

S.St.J. WARNE

Department of Geology, University of Newcastle, Shortland, N.S.W. 2308 (Australia)

J.V. DUBRAWSKI

BHP Central Research Laboratories, P.O. Box 188, Wallsend, N.S.W. 2287 (Australia)

(Received 20 October 1986; in final form 7 January 1987)

ABSTRACT

The newly established technique of high-temperature DSC has provided a method for the determination of the decomposition enthalpies of members of the dolomite–ferroan dolomite–ankerite series. The minerals studied in nitrogen included dolomite, containing no iron, and members substituted by iron in the mole fraction range 0.082–0.49. A linear decrease in enthalpy was observed with increasing iron substitution. Measurements were sensitive to technique and values were low if sample cups were uncovered. Products from the thermal decomposition of the carbonates were examined by powder X-ray diffraction. Applications are to mineralogy and coal science.

INTRODUCTION

The dolomite group of trigonal carbonates which has the general formula $AB(CO_3)_2$ (where A = Ba, Ca; and B = Fe^{2+}, Mg, Mn, Ca) contains the isomorphous substitution series dolomite–ferroan dolomite–ankerite, where, in the B position Fe^{2+} becomes progressively substituted for Mg in the dolomite [$CaMg(CO_3)_2$] structure.

Minerals, particularly from the low-iron dolomite–ferroan dolomite end of this series, are widely used in industry where the Fe content is important and often deleterious. Differential thermal analysis has proved particularly valuable for the semiquantitative evaluation of such Fe contents [14].

However, with the advent of high-temperature DSC (to temperatures of 950–1000 °C +) the way has been opened for the rapid quantitative determinations of small samples. Such data are directly applicable to improved

* Dedicated to Professor W.W. Wendlandt on the occasion of his 60th birthday.

0040-6031/87/$03.50

TABLE 1

Chemical analysis of the dolomite–ankerite mineral series (%)

Sample [a]	CaO	FeO	MnO	MgO	CO_2	Total
1. Dolomite: $Ca_{1.028}Mn_{0.0016}Mg_{0.970}(CO_3)_2$	30.78	–	0.06	20.88	46.99	98.71
2. Ferroan dolomite: $Ca_{0.978}Fe_{0.0816}Mn_{0.012}Mg_{0.929}(CO_3)_2$	29.00	3.10	0.46	19.80	46.56	98.92
3. Ferroan dolomite: $Ca_{1.053}Fe_{0.145}Mn_{0.036}Mg_{0.767}(CO_3)_2$	30.87	5.43	1.32	16.16	46.02	99.80
4. Ferroan dolomite: $Ca_{1.017}Fe_{0.226}Mn_{0.059}Mg_{0.698}(CO_3)_2$	29.43	8.37	2.15	14.52	45.41	99.88
5. Ankerite: $Ca_{1.024}Fe_{0.417}Mn_{0.031}Mg_{0.529}(CO_3)_2$	28.83	15.02	1.09	10.70	44.18	99.82
6. Ankerite: $Ca_{0.997}Fe_{0.418}Mn_{0.032}Mg_{0.553}(CO_3)_2$	28.13	15.11	1.12	11.21	44.28	99.85
7. Ankerite: $Ca_{1.037}Fe_{0.490}Mn_{0.019}Mg_{0.454}(CO_3)_2$	28.93	17.51	0.67	9.11	43.78	100.00

[a] Carbonate minerals 1–7 are from: 1, British chemical standard dolomite (BCS 368); 2, Kalgoorlie, W. Australia; 3, Wallaroo, S. Australia; 4, Tintagel, England; 5, Teruel, Spain; 6, Gollrad Mürzsteg, Styria; and 7, Blue Rock Tunnel, PA, U.S.A.

Fe content determinations and the quantification of endothermic enthalpy effects caused by increasing Fe contents. For these carbonates the former is important where Fe contents are deleterious for industrial uses and the latter reduces the endothermic heat-robbing decomposition reactions they undergo during combustion in energy coals or during oil shale retorting.

EXPERIMENTAL

All DSC curves were recorded on a Rigaku Denki Thermoflex 8100 series instrument consisting of TG, DTA and DSC modular units. The DSC unit possessed a range of ± 0.5 to 16 mcal s^{-1} and was operative to about 950 °C. Samples were heated in platinum cups, with or without polished platinum lids. Calcined alumina was used as the thermal reference material. Experiments were carried out in high-purity flowing nitrogen (200 ml min^{-1}).

Calibration of the instrument was done using a series of simple salts (ICTA standards) as described earlier [1]. The "instrument parameter" K was determined over the temperature range 400–900 °C.

The mineral carbonates studied belong to the dolomite–ferroan dolomite–ankerite series, for which chemical analyses were obtained as shown in Table 1. All samples were reduced to -50 μm particle size prior to thermal analysis. Sample masses throughout were in the range 5–50 mg and the heating rate was 10 °C min^{-1}. Chart speed was maintained within the range 5–20 mm min^{-1}. Peak areas were measured using a Tamaya Planix 7 planimeter.

Calculated heats of reaction for the mineral dolomite were obtained from data stored in the CSIRO-SGTE Thermodata system. Measured enthalpies were obtained from the equation

$$\Delta HM = KA \qquad (1)$$

where ΔH is the energy (mJ mg^{-1}) for a given process, M the sample mass (mg), K the "instrumental parameter" and A the peak area normalised to energy values.

X-ray diffraction patterns were recorded on a Siemens D-500 diffractometer using Cu $K\alpha$ radiation and a graphite monochromator. Data were collected in the step-scan mode employing a 0.02° 2θ step-size and a 1 s counting time per step, over the range 5–70° 2θ.

RESULTS AND DISCUSSION

DSC curves and powder diffraction patterns

Decomposition of the minerals belonging to the dolomite–ankerite series was carried out in flowing nitrogen since oxidation of the iron constituents is

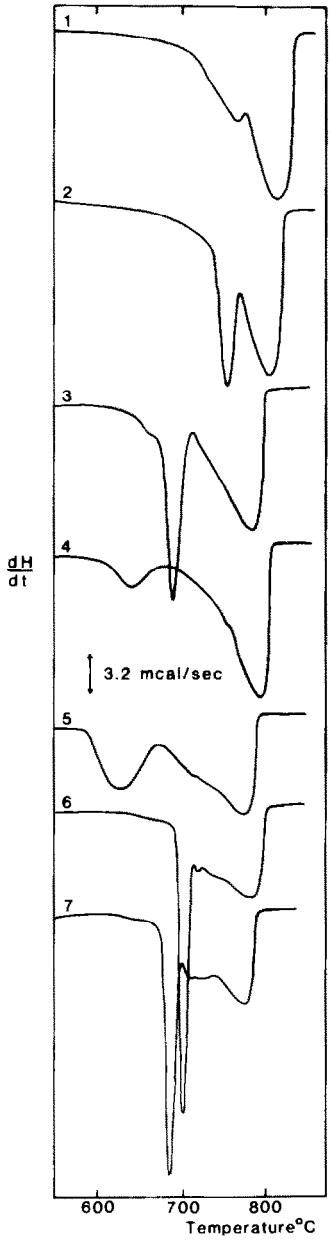

Fig. 1. DSC curves of seven members of the dolomite–ankerite series determined with lids in flowing N_2 illustrating the effects produced with increasing Fe contents, i.e. from curves 1–7 (see Table 1 for chemical analyses). Sample masses used were 22.25, 23.27, 24.62, 21.85, 24.22, 21.97 and 22.61 mg, respectively.

known to occur in air [2,3]. DSC curves of the dolomite and ankerite minerals are shown in Fig. 1. The DTA curve for dolomite is well known and consists essentially of two endothermic peaks. The lower-temperature

TABLE 2

Peak temperatures for the decomposition of dolomite–ferroan dolomite–ankerite mineral series

Sample	Peak temp. (°C)
1. Dolomite $Ca_{1.028}Mn_{0.0016}Mg_{0.970}(CO_3)_2$	760, 820
2. Ferroan dolomite $Ca_{0.978}Fe_{0.0816}Mn_{0.012}Mg_{0.929}(CO_3)_2$	755, 800
3. Ferroan dolomite $Ca_{1.053}Fe_{0.145}Mn_{0.036}Mg_{0.767}(CO_3)_2$	690, 725sh [a], 790
4. Ferroan dolomite $Ca_{1.017}Fe_{0.226}Mn_{0.059}Mg_{0.698}(CO_3)_2$	645, 755, 800
5. Ankerite $Ca_{1.024}Fe_{0.417}Mn_{0.031}Mg_{0.529}(CO_3)_2$	615, 700, 750
6. Ankerite $Ca_{0.997}Fe_{0.418}Mn_{0.032}Mg_{0.553}(CO_3)_2$	700, 715, 740, 780
7. Ankerite $Ca_{1.037}Fe_{0.490}Mn_{0.019}Mg_{0.454}(CO_3)_2$	680, 700, 725, 775

[a] sh = shoulder temperature.

peak is believed to be associated with breakdown of the magnesium carbonate component, the higher temperature with the remaining calcium carbonate component. However, the mechanism appears to be complex and not fully understood [4–7]. Substitution by iron causes changes in the thermal behaviour of the resulting ferroan dolomite–ankerites. Their DTA curves have been reported previously and generally show at least three endothermic peaks [8–14]. Improved resolution, resulting in complete peak separation, results when ankerites are heated in flowing carbon dioxide [14].

The overall appearance of the DSC curves is similar to that of DTA curves already reported. Essentially three peaks are obtained which are not completely resolved so that it is difficult to follow the change in any one due to changes in iron content (Fig. 1). It has been reported by Warne et al. [14] that in flowing carbon dioxide the first endotherm shifts to lower temperatures as the mole fraction of iron increases. From Table 2 it is apparent that this trend is followed only part-way with the DSC curves determined in N_2. From dolomite, and with increasing iron, the peak temperature decreases until ferroan dolomite samples (6) and (7). Then the peak temperature rises. Both these samples yielded curves characteristically different from the rest, with intense and sharp first peak endotherms (cf. curves 1–7 Fig. 1).

The products of thermal decomposition were examined by X-ray diffraction as shown in Fig. 2. The formation of dicalcium ferrite, $2CaO \cdot Fe_2O_3$, is apparent in all samples except the least substituted dolomite, and increases with iron content as might be expected. Milodowski and Morgan [15] have reported this phase being formed during the breakdown of ferroan

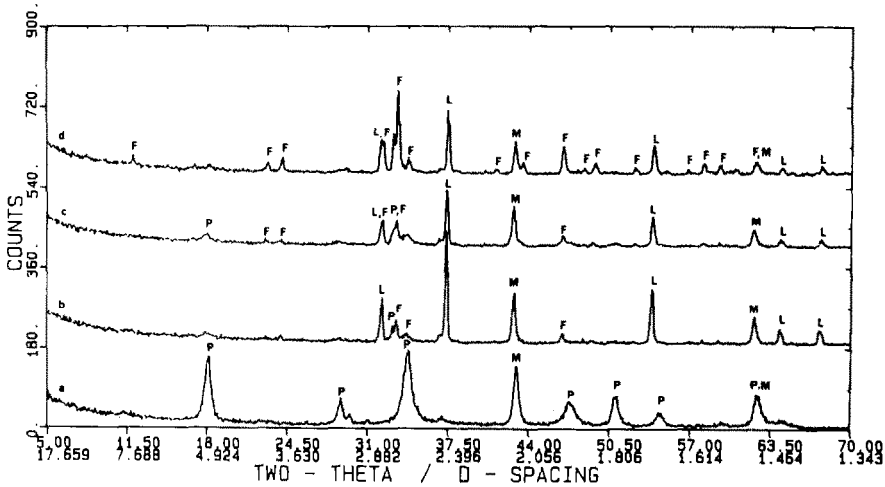

Fig. 2. X-ray diffraction patterns of the products of thermal decomposition of the dolomite–ankerite series carbonates. (a) Ferroan dolomite 2; (b) ferroan dolomite 3; (c) ferroan dolomite 4; (d) ankerite 5. Phases identified: (F) $2CaO \cdot Fe_2O_3$; (L) CaO; (M) MgO; (P) $Ca(OH)_2$.

dolomite–ankerites in flowing carbon dioxide. However, we observed the position of several ferrite diffraction peaks to be uniformly shifted by about 0.03 Å, suggesting the possibility of substitution. The most likely source was magnesium which indicated that $2CaO \cdot MgO \cdot Fe_2O_3$ might also be involved. This has been identified by Iwafuchi et al. [13] and Stadler [9] in the final products of the thermal breakdown of ferroan-dolomites. As Fig. 2 shows, all patterns contained diffraction peaks due to MgO, CaO and, in varying amounts, its hydrolysed product $Ca(OH)_2$.

Measurement of enthalpy values and the effect of substitution

It was observed that the DSC curves were affected by experimental technique. Figure 3 (curves 3 and 4) shows the curve for dolomite varied according to whether the sample was heated in a cup with or without a platinum lid. The single asymmetric endotherm splits into two distinct peaks when the sample is covered. The substituted carbonates behave similarly (Fig. 3, curves 1 and 2). The first endotherm moves to a lower temperature, the last to a higher temperature, and those between are resolved further. These effects arise due to the localised increase in partial pressure of CO_2 during decomposition, which separates the peaks in a manner akin to the behaviour of ankerites heated in flowing carbon dioxide, as mentioned above [14].

More importantly, the peak areas were altered by this difference in technique. Figure 4 illustrates the linear relationship between peak area and

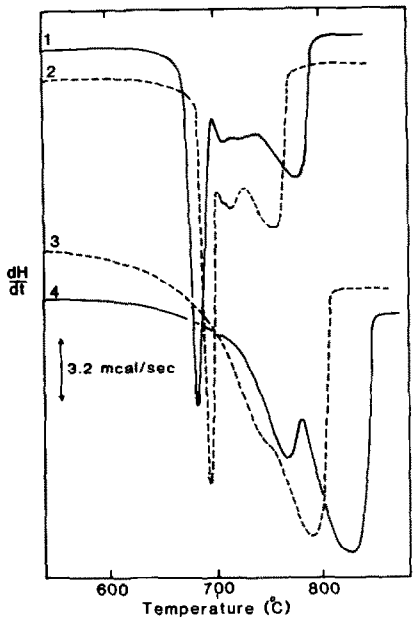

Fig. 3. DSC curves of dolomite and ankerite determined in flowing N_2 to illustrate the different effects produced with (———) and without (- - - - -) lids. (1), (2) Ankerite 7; (3), (4) dolomite 1.

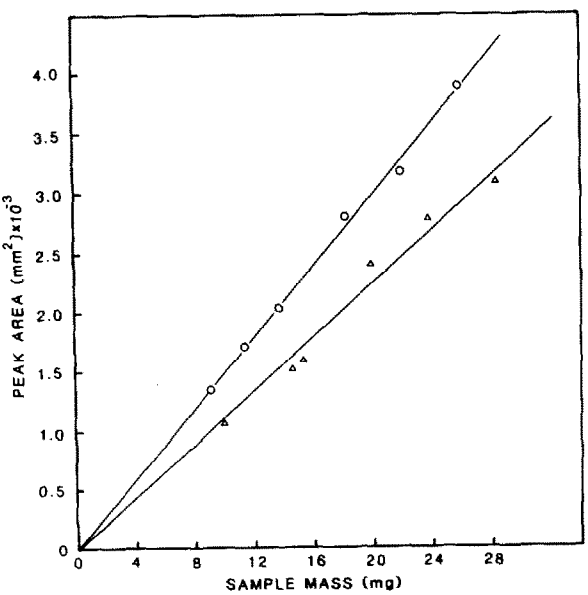

Fig. 4. Plot of ankerite 6 total peak area versus sample mass for DSC curves determined in flowing N_2 from samples heated with (○) and without (△) lids.

TABLE 3

Enthalpy values for the decomposition in nitrogen of members of the dolomite–ferroan dolomite–ankerite series (b, Pt cups with lids; c, Pt cups without lids)

Sample	Mole fraction		ΔH (kJ mol^{-1})	
	Fe	Mg	b	c
1. Dolomite [a] $Ca_{1.028}Mn_{0.0016}Mg_{0.970}(CO_3)_2$	–	0.970	290 ± 6	243
2. Ferroan dolomite $Ca_{0.978}Fe_{0.0816}Mn_{0.012}Mg_{0.929}(CO_3)_2$	0.0816	0.929	270 ± 8	232
3. Ferroan dolomite $Ca_{1.053}Fe_{0.145}Mn_{0.036}Mg_{0.767}(CO_3)_2$	0.145	0.767	267 ± 8	–
4. Ferroan dolomite $Ca_{1.017}Fe_{0.226}Mn_{0.059}Mg_{0.698}(CO_3)_2$	0.226	0.698	264 ± 6	224
5. Ankerite $Ca_{1.024}Fe_{0.417}Mn_{0.031}Mg_{0.529}(CO_3)_2$	0.417	0.529	253 ± 5	–
6. Ankerite $Ca_{0.997}Fe_{0.418}Mn_{0.032}Mg_{0.553}(CO_3)_2$	0.418	0.553	250 ± 5	208
7. Ankerite $Ca_{1.037}Fe_{0.490}Mn_{0.019}Mg_{0.454}(CO_3)_2$	0.490	0.454	247 ± 2	190

[a] Calculated $\Delta H = 296$ kJ mol^{-1}.

sample mass for ankerite 6 (Table 1). Two lines of different slope are obtained depending upon the presence and absence of a lid. It was found that the slope is always smaller when the lid is absent and a poorer line of best fit is obtained. Radiation and thermal losses from evolving CO_2 occur in uncovered samples and produce lower enthalpy values. With the sample covered by a polished lid, heat losses are minimised. Table 3 shows that the agreement between calculated and measured values for dolomite is good when the sample is covered, but that the measured value is about 20% lower than theoretical when the sample is uncovered.

The enthalpies of decomposition, ΔH, were obtained from eqn. (1) using averaged K values. This was considered a reasonable procedure as K varied between 1.25 and 1.35 for the 100 °C spread of the unresolved peaks. Figure 5 shows the increase in peak area per unit mass for several members of the series. Dolomite produced the highest slope, ferroan dolomite was intermediate, and the lowest value was shown by ankerite containing the highest iron content (see Table 1, samples 1, 4 and 7, for chemical analyses showing increasing iron substitution).

The calculated ΔH values are shown in Table 3. It can be seen that they decrease by ~ 45 kJ mol^{-1} across the series with increasing iron content. Conversely, ΔH increases with increasing magnesium substitution. Plots of mole fractions of iron and magnesium against ΔH are shown in Fig. 6. Although the trend in enthalpy values is clear, the error in the precision of measurement is such as to preclude a clear distinction between small

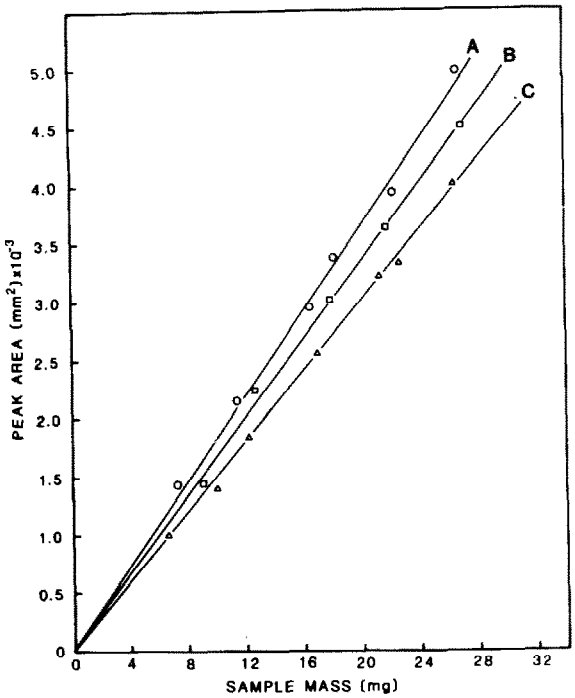

Fig. 5. Plot of total peak area versus sample mass for DSC curves determined in flowing N_2. (A) Dolomite 1, (B) ferroan dolomite 4 and (C) ankerite 7. Chemical compositions are shown in Table 1.

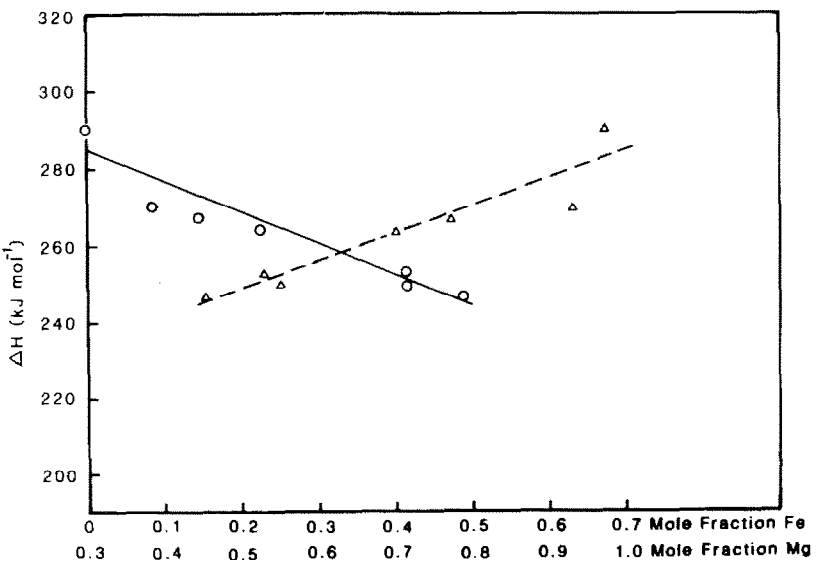

Fig. 6. Plots of ΔH values versus (○) Fe and (△) Mg contents from the data in Table 3.

changes in substitution. However, it is possible to separate dolomites containing, say, 0.1 and 0.4 mole fractions of iron or magnesium by their enthalpies.

It is also apparent that several enthalpy values, particularly those due to dolomites containing low iron contents, do not sit firmly on the line in Fig. 6 and are too low. This is particularly true for the first member, $Ca_{0.978}Fe_{0.0816}Mn_{0.012}Mg_{0.929}(CO_3)_2$. A possible explanation is the presence of substituted manganese, which, at low levels of iron, is present in a comparable ratio. As a result, several of the early members may behave as ferroanmanganoan dolomites and therefore yield enthalpies in keeping with this series. Iwafuchi et al. [13] have reported the behaviour of ferroanmanganoan dolomites in CO_2 and shown that their behaviour is quite complex, involving the formation of ferromanganoan oxides.

CONCLUSIONS

A number of conclusions can be drawn. Firstly, that DSC can be employed to measure the enthalpies of substituted mineral species and is valuable in providing ΔH values that cannot be conveniently calculated or are otherwise unavailable. Significantly lower determinations occur, however, if thermal losses are not eliminated. Secondly, DSC can quantitatively establish the thermal effect of iron substitution within the dolomite–ankerite series. Earlier work [14] involving DTA had qualitatively demonstrated this effect. Finally, the resolution of DTA curves for members of this series in flowing CO_2 should be equally successful with DSC. Complete separation of the second endotherm, which is directly linked to iron substitution, would result and could be measured independently of the overall enthalpy value. This approach is currently being undertaken and will be reported in due course.

ACKNOWLEDGEMENTS

The authors wish to acknowledge the technical assistance of Ms. S. Bell and the support of The Broken Hill Proprietary Company Ltd.

REFERENCES

1 J.V. Dubrawski and S.St.J. Warne, Thermochim. Acta, 104 (1986) 77.
2 R.C. Mackenzie (Ed.), Differential Thermal Analysis, Academic Press, London, 1970, Vol. 1, p. 323.
3 S.St.J. Warne, in C. Karr, Jr. (Ed.), Analytical Methods for Coal and Coal Products, Vol. III, Academic Press, London, 1979, pp. 447–477.

4 R. Otsuka, Thermochim. Acta, 100 (1986) 69.
5 R.A.W. Haul and H. Heysteck, Am. Mineral., 37 (1952) 166.
6 W.R. Bandi and G. Krapf, Thermochim. Acta, 14 (1976) 221.
7 R. Otsuka, S. Tanabe and K. Iwafuchi, J. Miner. Metall. Inst. Jpn., 96 (1980) 581.
8 J.L. Kulp, P. Kent and P.F. Kerr, Am. Mineral., 36 (1951) 643.
9 H.A. Stadler, Schweiz. Mineral. Petrogr. Mitt., 44 (1964) 187.
10 W. Smykatz-Kloss, Beitr. Mineral. Petrogr., 9 (1964) 481.
11 C.W. Beck, Am. Mineral., 35 (1950) 985.
12 R. Otsuka and N. Imai, J. Miner. Metall. Inst. Jpn., 84 (1968) 203 (in Japanese).
13 K. Iwafuchi, C. Watanabe and R. Otsuka, Thermochim. Acta, 66 (1983) 105.
14 S.St.J. Warne, D.J. Morgan and A.E. Milodowski, Thermochim. Acta, 51 (1981) 105.
15 A.E. Milodowski and D.J. Morgan, in D. Dollimore (Ed.), Proc. 2nd ESTA Conf., Aberdeen, 1981, Heydon, London, pp. 468–471.